

Article

Tedaniophorbasins A and B—Novel Fluorescent Pteridine Alkaloids Incorporating a Thiomorpholine from the Sponge *Tedaniophorbas ceratosis*

Asadhawut Hiranrat^{1,2,3,†}, Darren C. Holland^{1,4} , Wilawan Mahabusarakam^{2,3}, John N. A. Hooper^{4,5} , Vicky M. Avery^{4,6}  and Anthony R. Carroll^{1,4,*} 

¹ School of Environment and Science, Griffith University, Gold Coast, QLD 4222, Australia; hasadhawut@tsu.ac.th (A.H.); darren.holland@griffithuni.edu.au (D.C.H.)

² Department of Chemistry, Faculty of Science, Prince of Songkla University, Hat Yai, Songkhla 90112, Thailand; wilawan.m@psu.ac.th

³ Natural Products Research Center, Faculty of Science, Prince of Songkla University, Hat Yai, Songkhla 90112, Thailand

⁴ Griffith Institute for Drug Discovery Institute, Griffith University, Brisbane, QLD 4111, Australia; john.hooper@qm.qld.gov.au (J.N.A.H.); v.avery@griffith.edu.au (V.M.A.)

⁵ Queensland Centre for Biodiversity, Queensland Museum, South Brisbane, QLD 4101, Australia

⁶ Discovery Biology, Griffith University, Nathan, QLD 4111, Australia

* Correspondence: a.carroll@griffith.edu.au; Tel.: +61-7-5552-9187; Fax: +61-7-5552-9047

† Current address: Department of Chemistry, Thaksin University, Paphayom, Phatthalung 93210, Thailand.



Citation: Hiranrat, A.; Holland, D.C.; Mahabusarakam, W.; Hooper, J.N.A.; Avery, V.M.; Carroll, A.R.

Tedaniophorbasins A and B—Novel Fluorescent Pteridine Alkaloids Incorporating a Thiomorpholine from the Sponge *Tedaniophorbas ceratosis*.

Mar. Drugs **2021**, *19*, 95. <https://doi.org/10.3390/md19020095>

Academic Editors: Vassilios Roussis; Sylvain Petek and Cécile Debitus

Received: 3 January 2021

Accepted: 3 February 2021

Published: 7 February 2021

Publisher's Note: MDPI stays neutral with regard to jurisdictional claims in published maps and institutional affiliations.



Copyright: © 2021 by the authors. Licensee MDPI, Basel, Switzerland. This article is an open access article distributed under the terms and conditions of the Creative Commons Attribution (CC BY) license (<https://creativecommons.org/licenses/by/4.0/>).

Abstract: Two new fluorescent pteridine alkaloids, tedaniophorbasins A (1) and B (2), together with the known alkaloid *N*-methyltryptamine, were isolated, through application of mass directed purification, from the sponge *Tedaniophorbas ceratosis* collected from northern New South Wales, Australia. The structures of tedaniophorbasins A and B were deduced from the analysis of 1D/2D NMR and MS data and through application of ¹³C NMR DFT calculations. Tedaniophorbasin A possesses a novel 2-imino-1,3-dimethyl-2,3,7,8-tetrahydro-1H-[1,4]thiazino[3,2-g]pteridin-4(6*H*)-one skeleton, while tedaniophorbasin B is its 2-oxo derivative. The compounds show significant Stokes shifts (~14,000 cm⁻¹) between excitation and emission wavelengths in their fluorescence spectra. The new compounds were tested for bioactivity against chloroquine-sensitive and chloroquine-resistant strains of the malaria parasite *Plasmodium falciparum*, breast and pancreatic cancer cell lines, and the protozoan parasite *Trypanosoma brucei brucei* but were inactive against all targets at 40 μM.

Keywords: sponge; *Tedaniophorbas ceratosis*; pteridine alkaloids; fluorescence; tedaniophorbasin A; malaria

1. Introduction

Chemical diversity has been correlated with biological activity, and the structural diversity of natural products is more like that observed in drugs compared to synthetic libraries [1]. It has also been well documented that the marine environment is a source of unique structural motifs or scaffolds absent in species from the terrestrial environment or in synthetic libraries [2,3]. These novel scaffolds also contain a higher percentage of nitrogen atoms relative to carbon and oxygen compared to scaffolds derived from terrestrial sources [4]. This makes the marine environment a preferred source for biodiscovery. The northern coast of New South Wales in eastern Australia is a biogeographic transition zone in the south-west Pacific that is represented by marine species from both tropical and temperate regions [5]. Little is known about the sessile marine invertebrate (apart from corals) biodiversity of this region, and consequently there has been very little natural product chemistry reported for species collected from this location [6]. Due to the paucity of chemical data reported for species from this region, we have initiated a project to investigate

the chemical diversity in relation to the sessile marine invertebrate biodiversity of the region. To date, we have collected over 500 sponges, ascidian, and bryozoan specimens from reefs from this region, and a systematic analysis of the chemistry they contain has been initiated [7–12]. Herein, we report on the isolation, structure determination, and biological activity of two new alkaloids, tedaniophorbasins A (**1**) and B (**2**), possessing a novel skeleton (Figure 1) that we have isolated from *Tedaniophorbas ceratosis* collected from oceanic waters adjacent to Cook Island in far northern New South Wales, Australia. This is the first report on the chemistry of sponges from the genus *Tedaniophorbas*.

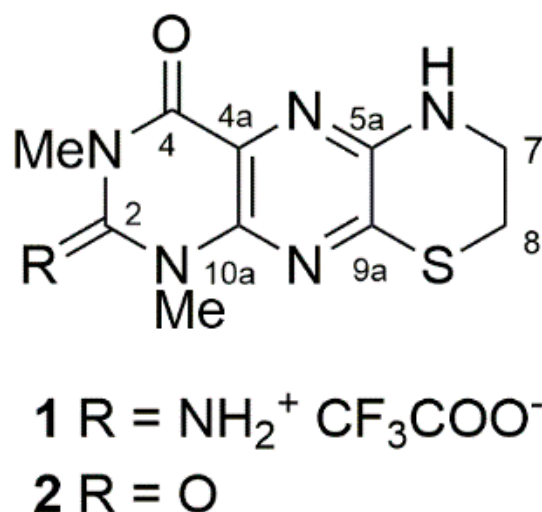


Figure 1. Chemical structures of tedaniophorbasin A (**1**) and B (**2**) isolated from the Australian sponge *Tedaniophorbas ceratosis*.

2. Results and Discussion

The frozen sponge was chopped into small pieces and extracted by repeated sonication in MeOH. The MeOH extracts were combined and evaporated, and the yellow brown residue was adsorbed onto C₁₈ silica gel. The extract-impregnated gel was separated by preparative HPLC on C₁₈-bonded silica gel with a gradient from 1% aqueous TFA to MeOH containing 1% TFA with one min. timed fractions collected. These fractions were further analyzed by (+)-LRESIMS, and only two groups of fractions (fraction 17–20 and fraction 27) showed prominent ions by MS. Fractions 17 and 18 had ion peaks at *m/z* 175 and 265, fractions 19 and 20 had an ion peak at *m/z* 175 and fraction 27 had an ion peak at *m/z* 266. These fractions were evaporated and analyzed by ¹H NMR spectroscopy. Fractions 17 and 18 contained a mixture of **1** and *N*-methyltryptamine. These compounds were separated from each other by recrystallization from MeOH. The supernatant was pure *N*-methyltryptamine, and **1** was obtained as fine needles (18.5 mg, 0.09%). Fractions 19 and 20 were pure *N*-methyltryptamine (34.7 mg, 0.17%) and fraction 27 was pure **2** (1.3 mg, 0.007%).

Tedaniophorbasin A (**1**) was isolated as fluorescent yellow needles as its TFA salt. Positive HRESIMS measurement of the MH⁺ peak (at *m/z* 265.0863 (Δ −1.2 ppm)) established a molecular formula of C₁₀H₁₂N₆OS for **1**, inferring that it contained eight degrees of unsaturation. The IR spectrum of **1** had absorption bands at 1712 and 1679 cm^{−1}, suggesting that it contained amide and aromatic groups. The UV spectrum had absorption maxima at 223, 280, 296, and 419 nm, indicating that **1** contained an extended aromatic chromophore. Excitation at the absorption maxima at 280 and 419 nm led to intense fluorescence at 490 nm (Figure 2).

The ¹H NMR spectrum of **1** (Table 1) was very simple, with only six resonances being observed. Edited HSQC correlations (Figure S5) indicated that two of the proton singlets could be assigned to *N*-methyl groups δ_{H/C} 3.66/31.3 and 3.46/30.3 and two were methylene groups δ_{H/C} 3.65/40.6 and 3.34/26.3, while the remaining two signals were due

to protons that were not attached to carbons. COSY correlations (Figure S4) between the methylene resonance at δ_{H} 3.65 and both the methylene resonance at δ_{H} 3.34 and an amine signal at δ_{H} 8.15 indicated that a $\text{CH}_2\text{CH}_2\text{NH}$ moiety was present in the molecule. The ^1H and ^{13}C chemical shifts for the methylene at 3.34/26.3 were consistent with it being substituted by a sulfur atom [13].

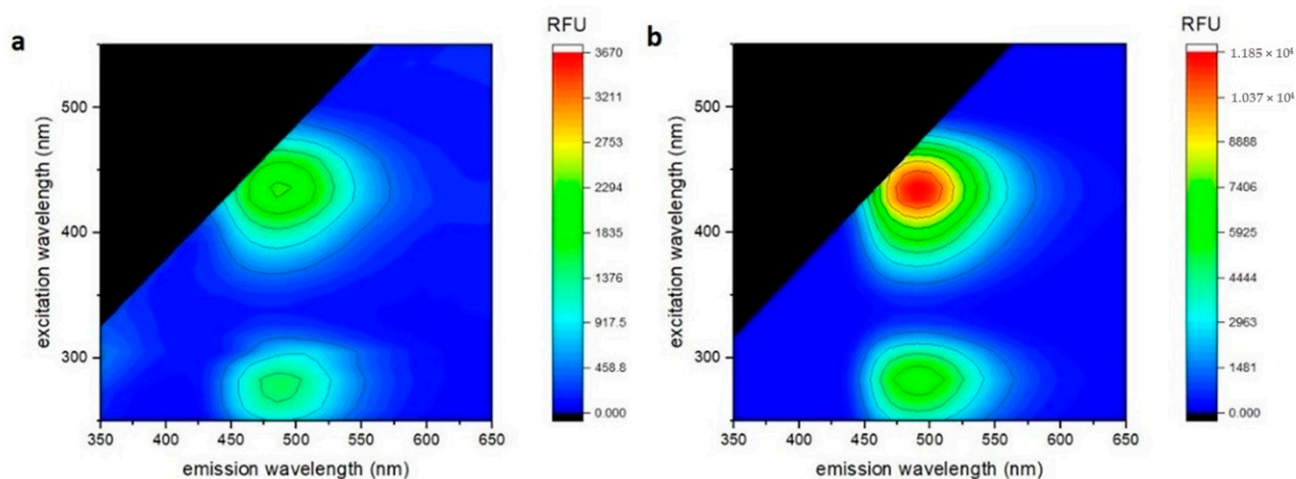


Figure 2. 3D fluorescence spectra of tedaniophorbins A (a) and B (b).

Table 1. NMR data for tedaniophorbins A and B (1 and 2) recorded in $\text{DMSO } d_6$ at 30°C ^a.

Position	δ_{C} , Type	1		2	
		δ_{H} , Mult. (J in Hz)	δ_{C} , Type	δ_{H} , Mult. (J in Hz)	
1-NCH ₃	31.3, CH ₃	3.66, s	28.9, CH ₃	3.43, s	
2	151.0, C	-	150.0, C	-	
2-NH ₂ ⁺	-	9.05, bs	-	-	
3-NCH ₃	30.3, CH ₃	3.46, s	28.2, CH ₃	3.27, s	
4	157.4, C	-	159.9, C	-	
4a	120.6, C	-	123.6, C	-	
5a	148.0 ^b , C	-	146.6, C	-	
6	-	8.15, t (2.7)	-	7.64, t (2.7)	
7	40.6, CH ₂	3.65, m	40.7, CH ₂	3.61, m	
8	26.3, CH ₂	3.34, m	26.5, CH ₂	3.29, m	
9a	147.9 ^b , C	-	146.0, C	-	
10a	137.6, C	-	139.8, C	-	

^a Spectra recorded at 600 MHz for ^1H and 150 MHz for ^{13}C ; ^b assignments are interchangeable.

The ^{13}C NMR spectrum (Table 1, Figure S3) contained six additional signals not observed in the HSQC spectrum, and these could all be assigned to non-protonated sp^2 carbons. HMBC correlations (Figures S6–S8) from the *N*-methyl proton resonance at δ_{H} 3.66 to carbons at δ_{C} 151.0 and 137.6 and from the *N*-methyl proton resonance at δ_{H} 3.46 to carbons at δ_{C} 151.0 and 157.4 in combination with the presence of a two-proton broad singlet at δ_{H} 9.05 suggested that a 1,3-di-*N*-methylpyrimidin-2-imino-4-one moiety was present in the molecule. HMBC correlations from the two methylene proton resonances and the amine proton at δ_{H} 8.15 to the carbon resonances at δ_{C} 147.9/148.0 suggested that a disubstituted dehydrothiomorpholine was present in the molecule. The chemical shift of the remaining carbon signal at δ_{C} 120.6 was consistent with it being assigned to C-4a of the pyrimidine [13].

The degree of unsaturation derived from the molecular formula required two additional sp^2 nitrogen atoms to be present in the molecule. These atoms could only logically be placed between the pyrimidine and thiomorpholine partial structures, and six alternative structures (two pyrazine (1a/1a') and four pyridazines (1b/1b' and 1c/1c')) (Figure 3))

could be proposed, with three pairs of regioisomers about the thiomorpholino moiety being possible. Based on the observed chemical shifts, the four pyridazine structures were rejected. In the two pyridazine structures containing a C-C bond between C-4a and the thiomorpholine (structures **1b/1b'**), C-4a is predicted to be shielded and resonate at $\sim \delta_C$ 110 and C-10a deshielded, resonating at $\sim \delta_C$ 160, while in the two pyridazine structures with a C-C bond between C-10a and the thiomorpholino moiety (structures **1c/1c'**), C-4a and C-10a would both resonate at $\sim \delta_C$ 135 [13].

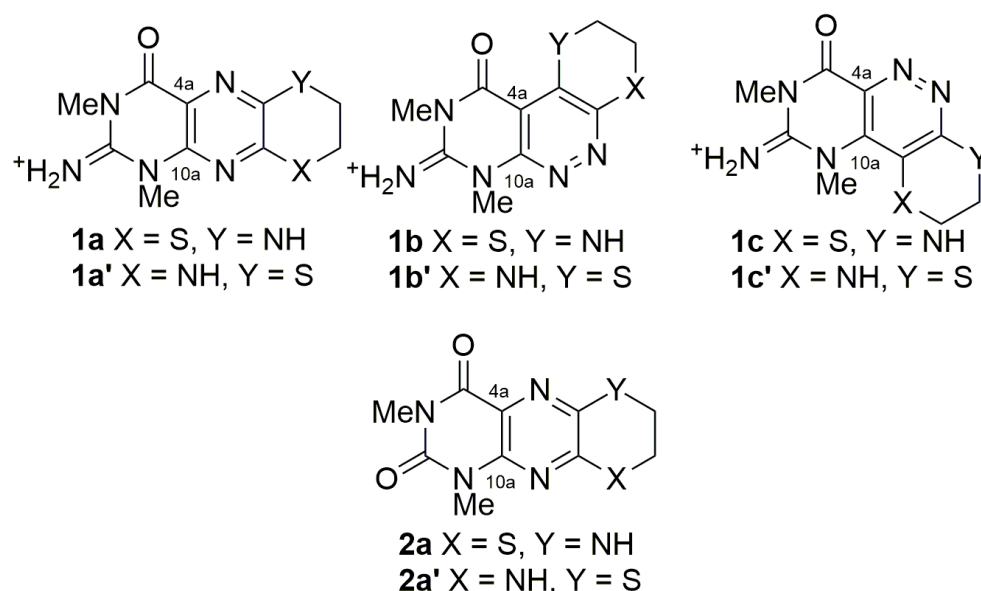


Figure 3. Six alternative structures for tedaniophorbacin A and two alternative structures for tedaniophorbacin B.

Comparison of the ^{13}C chemical shift data for C-2, C-4, C-4a, C-5a, C-9a, C-10a, 1-NCH₃, and 3-NCH₃ observed for **1** with equivalent carbons reported for the pteridine metabolites urochordamine A (**3**) isolated from the ascidian *Ciona savignyi* [14] and asteropterin (**4**) isolated from the sponge *Asteropus simplex* [15] provided convincing evidence that **1** contained a pyrazine moiety, since all carbons apart from C-4a and C-10a were within 3.5 ppm of those reported in **3**, while C-2, C-4a, C-5a, and C-10a were within 3.1 ppm of those reported in **4** (Figure 4).

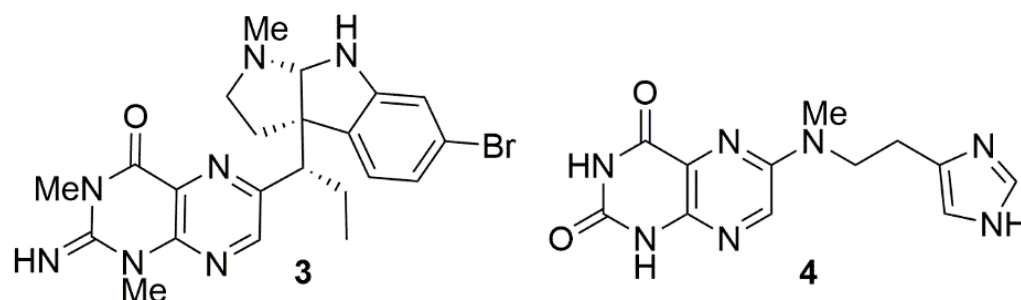


Figure 4. Marine pteridine natural products related to tedaniophorbacins A and B.

Unfortunately, the lack of pairs of protons proximal through space or protons within three bonds of more than one nitrogen atom meant that neither ROESY nor $^1\text{H}/^{15}\text{N}$ HMBC experiments would be useful to define the regiochemistry of the thiomorpholino moiety. Therefore, computational methods using density functional theory (DFT) GIAO-calculated ^{13}C NMR chemical shifts were used to predict the most probable isomer for **1** (structures **1a** or **1a'**). The DFT-calculated ^{13}C NMR isotropic shielding values were scaled to account for the heavy atom effect of sulfur [16] attached to C-8 and C-9a in **1a**, and C-5a

and C-7 in **1a'**, and compared with tedaniophorbasin A's (**1**) experimental ^{13}C NMR data. The DFT-calculated ^{13}C NMR data clearly indicated that structure **1a** (mean absolute error (MAE) = 1.8) containing the N and S atoms at positions 6 and 9, respectively, was a better match with **1**'s experimental ^{13}C NMR data compared with that obtained for the alternate structure **1a'** (MAE = 3.7, see supplementary material). The DFT-calculated ^{13}C NMR resonances in **1a'** with deviations >5.5 ppm were C-4, C-5a, and C-10a, whereas none of the calculated ^{13}C NMR resonances in **1a** deviated from the observed data by more than 3.6 ppm (Figure 5). Tedaniophorbasin A therefore possesses a novel 2-imino-1,3-dimethyl-2,3,7,8-tetrahydro-1*H*-[1,4]thiazino [3,2-*g*]pteridin-4(6*H*)-one skeleton.

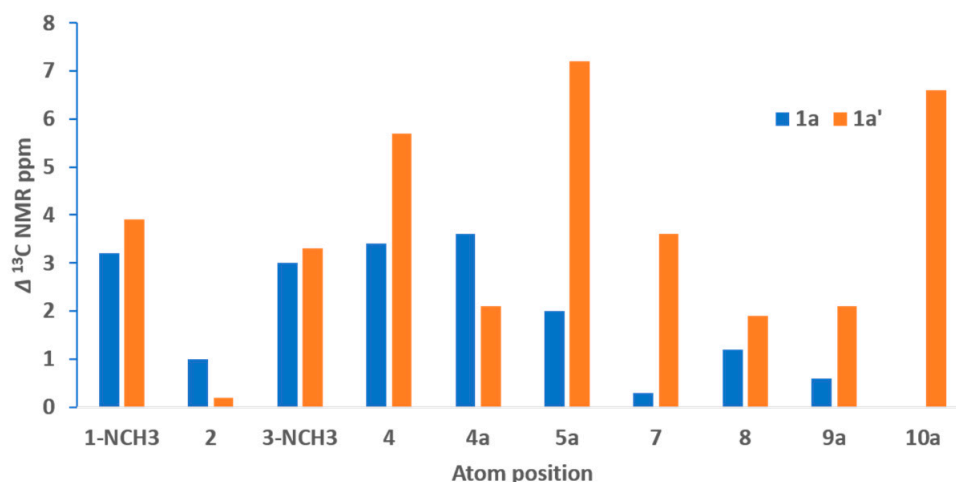


Figure 5. Calculated absolute ^{13}C NMR chemical shift deviations for density functional theory (DFT)-calculated δ_{C} compared to experimental δ_{C} for the two alternative regioisomers **1a** and **1a'** of tedaniophorbasin A.

Tedaniophorbasin B (**2**) was isolated as a fluorescent yellow gum. A mass ion (MH^+) at m/z 266.0706 (Δ 0 ppm) was consistent with **2** possessing a molecular formula of $\text{C}_{10}\text{H}_{11}\text{N}_5\text{O}_2\text{S}$. Its ^1H and ^{13}C NMR data (Table 1) were almost identical with that of **1**, with the most notable difference being the absence of the NH_2 resonance at δ_{H} 9.05. The COSY (Figure S13) (6-NH/7- CH_2 , 7- CH_2 /8- CH_2) and HMBC (Figures S15–S17) (1-NCH₃/C-2, C-10a; 3-NCH₃/C-2, C-4; 6-NH/C-8, C-9a; H-7/C-5a, C-8; and H-8/C-7, C-9a) correlation data for **2** was identical with that observed for **1**, indicating that the two molecules possessed the same molecular framework. Considering that the molecular formula for **2** differed from **1** by the replacement of a NH_2^+ with an oxygen, the most logical explanation is that **2** is the 2-oxo derivative of **1**. The structure proposed for tedaniophorbasin B (**2a**) is also supported by ^{13}C DFT (GIAO) NMR calculations (MAE = 1.3, compared to MAE = 3.2 for the 6-S, 9-NH regioisomer (**2a'**)) (see supplementary material). Tedaniophorbasin B is therefore the 2-oxo derivative of **1** and contains a novel 2-oxo-1,3-dimethyl-2,3,7,8-tetrahydro-1*H*-[1,4]thiazino[3,2-*g*]pteridin-4(6*H*)-one skeleton.

The tedaniophorbasins are structurally unique compounds, possessing a ring system that has not been reported either naturally or synthetically. The closest related structure is the synthetic 7,8-benzo derivative (**5**) prepared through reaction of 6,7-dichloro-1,3-dimethylumazine with 2-aminothiophenol (Figure 6) [17]. A similar reaction between mercaptoethylamine and 6,7-dichloro-1,3-dimethylumazine could yield tedaniophorbasin B (**2**). Marine pteridine alkaloids have previously been isolated from polychaete worms [18], sponges [15], ascidians [14,19], and fungi [20]. All previously reported marine pteridine alkaloids, however, have been unsubstituted at C-7, thus making the tedaniophorbasins the first C-7 substituted pteridines to be reported from a marine source. There have not been any previous chemical investigation of sponges from the genus *Tedaniophorbis*.

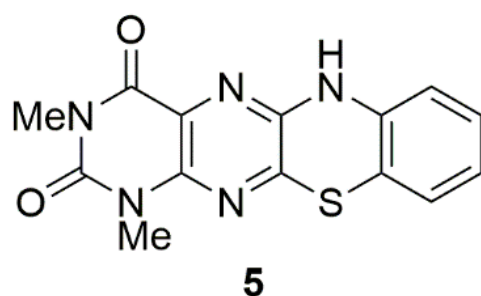


Figure 6. Most closely related synthetic pteridine derivative to the tedaniophorbins.

Tedaniophorbins A (**1**) and B (**2**) were tested for their ability to inhibit the growth of chloroquine-sensitive (3D7) and chloroquine-resistant (Dd2) strains of the malaria parasite *Plasmodium falciparum* [21], inhibition of the growth of the trypanosome *Trypanosoma brucei brucei* [22], and cytotoxicity towards pancreatic (Bx-PC-3, Panc-1, and Su-86-86) and breast cancer (BT-474, MCF-10A, and MDA-MB-231) cell lines [23] (assays that we routinely run in our labs), however, both compounds were inactive against all targets at the highest concentration (40 μ M) tested.

The lack of cellular bioactivity prompted us to question the ecological role for these intensely fluorescent molecules, since the intensely fluorescent yellow color of the sponge can be attributed to the tedaniophorbins. The fluorescence spectra for both **1** and **2** (Figure 2) showed significant Stokes shifts of $14,000\text{ cm}^{-1}$ (280 nm ex/490 nm em) and 3400 cm^{-1} (420 nm ex/490 nm em), suggesting excited state reactions and a change in dipole moments, respectively. The cyan fluorescence of tedaniophorbin A (**1**) and B (**2**) further suggests that the compounds might act as donor luminophores for bioluminescence, while their UV absorbance between 280 and 419 nm suggests a role as sunscreens, since both compounds absorb strongly in the UVA (315–400 nm) and UVB (280–315 nm) wavelength bands.

3. Materials and Methods

3.1. General Chemistry Experimental Procedures

NMR spectra were recorded at 30 °C on a Varian Inova 600 MHz NMR spectrometer (Pala Alto, CA, USA) equipped with a cryoprobe. Samples were dissolved in DMSO- d_6 , and the solvent peak was used as the reference at the chemical shifts δ_{H} 2.50 ppm and δ_{C} 39.52 ppm. LRESIMS data were recorded on a Water ZQ ESI mass spectrometer (Milford, MA, USA). (+)-High-resolution electrospray ionization mass spectrometry (HRESIMS) was used to determine the accurate molecular weight and molecular formula of the isolated compounds. HRESIMS were recorded on a Applied Biosystems Mariner Biospectrometry TOF workstation (Foster City, CA, USA) using positive electrospray ionization. Ultraviolet (UV) spectra were acquired on a Shimadzu UV-1800 UV spectrophotometer (Kyoto, Japan), and infrared (IR) measurements were recorded on a Bruker Tensor 27 spectrometer (Zürich, Switzerland). Fluorescence intensity spectra were recorded in MeOH by 3D top scanning on a Tecan Spark Plate Reader (Männedorf, Switzerland) with excitation wavelengths from 250 to 700 nm incremented by 10 nm and emissions intensity recorded from 280 to 700 nm at 10 nm steps at each excitation wavelength. HPLC separations were performed on a Merck Hitachi L-7100 pump equipped with a Hitachi L-7455 PDA detector, D-7000 interface (Tokyo, Japan), and a Gilson 215 liquid handler (Middleton, WI, USA) to collect the fractions. The guard column (20 mm \times 10 mm) was packed with Altech Davisil 30–40 μ m 60 Å C₁₈ silica gel (Columbia, MD, USA). The guard column was attached before the preparative column, a Thermo Fisher Scientific BetaSil C₁₈ (150 mm \times 21.2 mm, 5 μ m) (Waltham, MA, USA). The solvents used were HPLC grade MeOH (Lab-Scan) (Barcelona, Spain), Milli-Q PF (Sartorius, Göttingen, Germany) filtered water, and spectroscopy grade trifluoroacetic acid (TFA, Alfa Aesar) (Ward Hill, MA, USA).

3.2. Collections, Extraction, and Isolation

The sponge specimen *Tedaniophorbas ceratosis* (Ridley & Dendy, 1886) (Order: Poecilosclerida; Family: Acarnidae) (sp. number QM1179) was hand collected by SCUBA from Wommin Reef (10 m) just south of Cook Island, Northern NSW, Australia, in January 2010. A voucher specimen (QM G331842) is housed in the Queensland Museum. The specimen was identified by Dr. J. N. A. Hooper.

The sponge *Tedaniophorbas ceratosis* (20 g, wet weight) was chopped into small pieces and exhaustively extracted with MeOH (6 × 200 mL) in an ultrasonic bath (20 min. per extraction) to afford a yellow brown residue (0.892 g). This extract was then separated by reversed phase C₁₈ HPLC gradient elution from H₂O to MeOH (containing 1% TFA) over 60 min. and then eluted with MeOH (containing 1% TFA) for 10 min. to afford 70 fractions. Fractions 17 and 18 contained tedaniophorbasin A **1** and *N*-methyltryptamine, which were subsequently separated by recrystallization from MeOH. Tedaniophorbasin A (**1**) was crystallized from the solution to leave *N*-methyltryptamine in the supernatant. Fraction 20 eluting with 66% H₂O/34% MeOH yielded pure *N*-methyltryptamine, and fraction 27 eluting with 55% H₂O/45% MeOH (all containing 1% TFA) yielded pure tedaniophorbasin B (**2**).

Tedaniophorbasin A (**1**): yellow crystals (18.5 mg, 0.09%); m.p. 316 °C; UV (MeOH) λ_{max} (log ε) 223 (4.12), 280 (4.02), 296 (3.88), 419 (3.87) nm; IR ν_{max} (film) 3325, 3058, 2966, 2929, 1712, 1679, 1649, 1567, 1557, 1202, 1132 cm⁻¹; FLR (MeOH) λ_{ex} 280, λ_{em} 490 nm, λ_{ex} 419, λ_{em} 490 nm; ¹H and ¹³C NMR data, Table 1; (+) HRESIMS *m/z* 265.0863 (calcd for C₁₀H₁₃N₆OS, 265.0866).

Tedaniophorbasin B (**2**): yellow oil (1.3 mg, 0.007%); UV (MeOH) λ_{max} (log ε) 219 (4.01), 277 (3.77), 302 (3.57), 416 (3.55) nm; IR ν_{max} (film) 3302, 2918, 2850, 1679, 1200, 1135 cm⁻¹; FLR (MeOH) λ_{ex} 277, λ_{em} 490 nm, λ_{ex} 416, λ_{em} 490 nm; ¹H and ¹³C NMR data, Table 1; (+) HRESIMS *m/z* 266.0706 (calcd for C₁₀H₁₂N₅O₂S, 266.0706).

3.3. DFT ¹³C NMR Calculations

A thorough conformer search was performed on **1a**, **1a'**, **2a**, and **2a'** using MCMM with the OPLS3 forcefield within the Schrödinger MacroModel 2016 software suite operating on Windows 10. All conformers >21.0 kJ/mol from the energy minimum were discarded. The resultant conformational suites underwent DFT geometry optimization in the gas phase using the B3LYP/6-31G(d) functional and basis set in Gaussian 16 [24]. Modified python scripts based on the Willoughby protocol [25] were used to confirm that the geometry-optimized conformers were true energy minima and to confirm the absence of negative vibrational frequencies. The DFT (GIAO) ¹³C NMR shielding values were calculated on the geometry-optimized structures using the ωB97xD/6-31G(d) level of theory. The subsequent DFT isotropic shielding values were then Boltzmann averaged across each of the conformational suites [25] and scaled (with carbons attached to sulfur adjusted binomially) using the procedure reported by Kutateladze et al. [16]. Finally, the scaled ¹³C NMR chemical shifts for the structural isomers (**1a** and **1a'**; **2** and **2a'**) were analyzed using the sDP4+ method [26], however, the ωB97xD/6-31G(d) functional is not inherent to the Grimblat method, therefore a small amount of caution should be applied to this result (see supplementary material).

3.4. Biological Activity Testing

Biological profiling of compounds was undertaken using well-established protocols. Antiplasmodial activity was determined by testing compounds against chloroquine-sensitive (3D7) and chloroquine-resistant (Dd2) strains of *Plasmodium falciparum* as previously comprehensively described by Duffy and Avery [21].

Antitrypanosomal activity of compounds against *Trypanosoma brucei brucei* was undertaken as previously described by Sykes and Avery [22].

Evaluation of compounds for anti-proliferative activity against the breast cancer cell lines BT-474, MCF-10A, and MDA-MB-231 and pancreatic cell lines Bx-PC-3, Panc-1, and Su-86-86 was undertaken as described in detail by Lovitt et al. [23].

4. Conclusions

Analysis of a sponge *Tedaniophoras ceratosis* collected from the Australian south Pacific coast led to the isolation of two highly fluorescent alkaloids, tedaniophorbasins A and B. Both possess skeletons that are novel. Tedaniophorbasin A possesses a novel 2-imino-1,3-dimethyl-2,3,7,8-tetrahydro-1*H*-[1,4]thiazino[3,2-*g*]pteridin-4(6*H*)-one skeleton, while tedaniophorbasin B is the 2-oxo derivative of tedaniophorbasin A. Their structures were supported by comparison of experimental and DFT-calculated ^{13}C NMR data. Both compounds were inactive at 40 μM when tested for antiplasmodial, anticancer, and antitrypanosomal activity. This study highlights the fact that the south Pacific region contains marine genera that, to date, have not been investigated, and that these marine organisms hold the potential to contain novel chemistry. Future studies of south Pacific marine organisms will undoubtedly lead to further discoveries of novel chemistry.

Supplementary Materials: The following are available online at <https://www.mdpi.com/1660-3397/19/2/95/s1>: Figures S1–S8: ^1H NMR, ^{13}C NMR, COSY, HSQC, HMBC spectra of tedaniophorbasin A (1); Figures S10–S17: ^1H NMR, ^{13}C NMR, COSY, HSQC, HMBC spectra of tedaniophorbasin B (2). HRESIMS spectra for tedaniophorbasin A (1): Figure S9 and tedaniophorbasin B (2): Figure S18, Tables S1–S4 Calculated DFT (GIAO) ^{13}C NMR Chemical Shift for **1a**, **1a'**, **2a**, and **2a'** compared to experimental ^{13}C NMR data.

Author Contributions: Conceptualization: A.R.C. and A.H.; Methodology: A.H., A.R.C., D.C.H., and V.M.A.; Investigation: A.H., D.C.H., W.M., A.R.C., and J.N.A.H.; Funding acquisition: A.H., W.M., and A.R.C.; Supervision: A.R.C. and W.M.; Sponge ID: J.N.A.H.; Writing—review and editing: A.R.C., A.H., and D.C.H., All authors have read and agreed to the published version of the manuscript.

Funding: This research was partially funded by the Thailand Research Fund through the Royal Golden Jubilee Program for a travel scholarship awarded to A. Hiranrat (Grant No. PHD/0206/2549).

Data Availability Statement: The data presented in this study are available in the supplementary Materials file associate with this article.

Acknowledgments: The sponge was collected under the NSW DPI Fisheries Scientific collection permit P09/0031-1.1. We thank M. Sykes, S. Duffy, C. Lovitt, and T. Schelper, Griffith University, for their contributions to the antiplasmodial, cytotoxicity, and antitrypanosomal testing. The authors gratefully acknowledge Indy Siva and the Griffith University eResearch Services team for use of the 'Gowonda' High-Performance Computing (HPC) Cluster to calculate ^{13}C NMR data for **1** and **2**. The authors acknowledge the Australian Research Council (ARC) for support towards NMR equipment (Grants LE0668477, LE140100119, and LE0237908). We would like to acknowledge Griffith University for a scholarship for D.C.H.

Conflicts of Interest: The authors declare no conflict of interest. The funders had no role in the design of the study, in the collection, analyses, or interpretation of data, in the writing of the manuscript, or in the decision to publish the results.

References

1. Feher, M.; Schmidt, J.M. Property distributions: Differences between drugs, natural products, and molecules from combinatorial chemistry. *J. Chem. Inf. Comput. Sci.* **2003**, *43*, 218–227. [[CrossRef](#)] [[PubMed](#)]
2. Blunt, J.W.; Carroll, A.R.; Copp, B.R.; Davis, R.A.; Keyzers, R.A.; Prinsep, M.R. Marine Natural Products. *Nat. Prod. Rep.* **2018**, *35*, 8–53. [[CrossRef](#)]
3. Pye, C.R.; Bertinb, M.J.; Lokeya, R.S.; Gerwick, W.H.; Linington, R.G. Retrospective analysis of natural products provides insights for future discovery trends. *Proc. Natl. Acad. Sci. USA* **2017**, *114*, 5601–5606. [[CrossRef](#)]
4. Henkel, T.; Brunne, R.M.; Müller, H.; Reichel, F. Statistical Investigation into the Structural Complementarity of Natural Products and Synthetic Compounds. *Angew. Chem. Int. Ed.* **1999**, *38*, 643–647. [[CrossRef](#)]
5. Butler, A.J.; Rees, T.; Beesley, P.; Bax, N.J. Marine Biodiversity in the Australian Region. *PLoS ONE* **2010**, *5*, e11831. [[CrossRef](#)]

6. Carroll, A.R.; Copp, B.R.; Davis, R.A.; Keyzers, R.A.; Prinsep, M.R. Marine Natural Products. *Nat. Prod. Rep.* **2019**, *36*, 122–173. [[CrossRef](#)]
7. Carroll, A.R.; Wild, S.J.; Duffy, S.; Avery, V.M. Kororamide A, a new tribrominated indole alkaloid from the Australian bryozoan *Amathia tortuosa*. *Tetrahedron Lett.* **2012**, *53*, 2873–2875. [[CrossRef](#)]
8. Kleks, G.; Duffy, S.; Lucantoni, L.; Avery, V.M.; Carroll, A.R. Orthoscuticellines A–E, β -Carboline Alkaloids from the Bryozoan *Orthoscuticella ventricosa* Collected in Australia. *J. Nat. Prod.* **2020**, *83*, 422–428. [[CrossRef](#)] [[PubMed](#)]
9. Jennings, L.K.; Robertson, L.P.; Rudolph, K.E.; Munn, A.L.; Carroll, A.R. Anti-prion Butenolides and Diphenylpropanones from the Australian Ascidian *Polycarpa procera*. *J. Nat. Prod.* **2019**, *82*, 2620–2626. [[CrossRef](#)]
10. Kleks, G.; Holland, D.C.; Kennedy, E.K.; Avery, V.M.; Carroll, A.R. Antiplasmodial Alkaloids from the Australian Bryozoan *Amathia lamourouxii*. *J. Nat. Prod.* **2020**, *83*, 3435–3444. [[CrossRef](#)] [[PubMed](#)]
11. Jennings, L.J.; Prebble, D.W.; Xu, M.; Ekins, M.G.; Munn, A.L.; Mellick, G.D.; Carroll, A.R. Anti-prion and α -Synuclein Aggregation Inhibitory Sterols from the Sponge *Lamellosysidea cf. chlorea*. *J. Nat. Prod.* **2020**, *83*, 3751–3757. [[CrossRef](#)]
12. Hayton, J.H.; Grant, G.D.; Carroll, A.R. Three New Spongian Diterpenes from the Marine Sponge *Dendrilla rosea*. *Aust. J. Chem.* **2019**, *72*, 964–968. [[CrossRef](#)]
13. Pretsch, E.; Bühlmann, P.; Badertscher, M. *Structure Determination of Organic Compounds*, 4th ed.; Springer: Berlin/Heidelberg, Germany, 2009.
14. Tsukamoto, S.; Hirota, H.; Kato, H.; Fusetani, N. Urochordamines A and B: Larval Settlement/Metamorphosis-Promoting, Pteridine-Containing Physostigmine Alkaloids from the Tunicate *Ciona savignyi*. *Tetrahedron Lett.* **1993**, *34*, 4819–4822. [[CrossRef](#)]
15. Murayama, S.; Nakao, Y.; Matsunaga, S. Asteropterin, an inhibitor of cathepsin B, from the marine sponge *Asteropus simplex*. *Tetrahedron Lett.* **2008**, *49*, 4186–4188. [[CrossRef](#)]
16. Kutateladze, A.G.; Reddy, D.S. High-Throughput in Silico Structure Validation and Revision of Halogenated Natural Products Is Enabled by Parametric Corrections to DFT-Computed ^{13}C NMR Chemical Shifts and Spin-Spin Coupling Constants. *J. Org. Chem.* **2017**, *82*, 3368–3381. [[CrossRef](#)]
17. Abou-Hadeed, K.; Pfeleiderer, W. Pteridines eVIII Reactions of 6, 7-Dichloro-I, 3-dimethylumazine with Sulfur-Nucleophiles. *Pteridines* **1996**, *7*, 113–122. [[CrossRef](#)]
18. Kakoi, H.; Tanino, H.; Okada, K.; Inoue, S. 6-Acylumazines from the marine polychaete, *Odontosyllis undecimdonga*. *Heterocycles* **1995**, *41*, 789–797. [[CrossRef](#)]
19. Rudolph, K.E.; Liberio, M.S.; Davis, R.A.; Carroll, A.R. Pteridine-, thymidine-, choline- and imidazole-derived alkaloids from the Australian ascidian, *Leptoclinides durus*. *Org. Biomol. Chem.* **2013**, *11*, 261–270. [[CrossRef](#)]
20. You, M.; Liao, L.; Hong, S.H.; Park, W.; Kwon, D.I.; Lee, J.; Noh, M.; Oh, D.-C.; Oh, K.-B.; Shin, J. Lumazine Peptides from the Marine-Derived Fungus *Aspergillus terreus*. *Mar. Drugs* **2015**, *13*, 1290–1303. [[CrossRef](#)]
21. Duffy, S.; Avery, V.M. Development and optimization of a novel 384-well anti-malarial imaging assay validated for high-throughput screening. *Am. J. Trop. Med. Hyg.* **2012**, *86*, 84–92. [[CrossRef](#)]
22. Sykes, M.L.; Avery, V.M. Development of an Alamar Blue™ Viability Assay in 384-Well Format for High Throughput Whole Cell Screening of *Trypanosoma brucei brucei* Bloodstream Form Strain 427. *Am. J. Trop. Med. Hyg.* **2009**, *81*, 665–674. [[CrossRef](#)] [[PubMed](#)]
23. Lovitt, C.J.; Shelper, T.B.; Avery, V.M. Miniaturized three-dimensional cancer model for drug evaluation. *Assay Drug Dev. Technol.* **2013**, *11*, 435–448. [[CrossRef](#)] [[PubMed](#)]
24. Frisch, M.J.; Trucks, G.W.; Schlegel, H.B.; Scuseria, G.E.; Robb, M.A.; Cheeseman, J.R.; Scalmani, G.; Barone, V.; Petersson, G.A.; Nakatsuji, H.; et al. *Gaussian 16*; Gaussian Inc.: Wallingford, CT, USA, 2016.
25. Willoughby, P.H.; Jansma, M.J.; Hoye, T.R. A Guide to Small-Molecule Structure Assignment through Computation of (^1H and ^{13}C) NMR Chemical Shifts. *Nat. Protoc.* **2014**, *9*, 643–660. [[CrossRef](#)] [[PubMed](#)]
26. Grimblat, N.; Zanardi, M.M.; Sarotti, A.M. Beyond DP4: An Improved Probability for the Stereochemical Assignment of Isomeric Compounds Using Quantum Chemical Calculations of NMR Shifts. *J. Org. Chem.* **2015**, *80*, 12526–12534. [[CrossRef](#)]